STM JOURNALS

**Research and Reviews: Journal of Physics**
ISSN: 2278–2265(online), ISSN: 2347-9973(print)
Volume 5, Issue 2
www.stmjournals.com

# Third Order Perturbed Heisenberg Hamiltonian of BCC Ferromagnetic Ultra-Thin Films

***P. Samarasekara[1],*, N. U. S. Yapa[2]***
[1]Department of Physics, University of Peradeniya, Peradeniya, Sri Lanka
[2]Department of Physics, Open University of Sri Lanka, Kandy, Sri Lanka

***Abstract***

*For the first time, the solution of third order perturbed classical Heisenberg Hamiltonian equation with all the seven magnetic parameters including stress induced anisotropy and demagnetization factor is presented in this manuscript. Variation of third order perturbed total energy with applied in plane magnetic field, applied out of plane magnetic field, demagnetization factor and spin exchange interaction is described in this manuscript. Several peaks can be observed in each 3-D plot implying that there are many easy and hard directions for magnetization. All the simulations reported in this manuscript are given for a ferromagnetic film with three spin layers (N=3). Although this simulation was performed for some selected values of seven magnetic energy parameters, the simulation can be carried out for any values of magnetic energy parameters.*

***Keywords:*** *Perturbation, Heisenberg Hamiltonian, Ferromagnetic thin films*

****Author for Correspondence*** E-mail: pubudus@pdn.ac.lk

## INTRODUCTION

Ferromagnetic thin films find potential applications in magnetic memory devices and microwave devices. EuTe films with surface elastic stresses have been theoretically studied using Heisenberg Hamiltonian [1]. Magnetostriction of dc magnetron sputtered FeTaN thin films has been theoretically studied using the theory of De Vries [2]. Magnetic layers of Ni on Cu have been theoretically investigated using the Korringa-Kohn-Rostoker Green's function method [3]. Electric and magnetic properties of multiferroic thin films have been theoretically explained by modified Heisenberg and transverse Ising model using Green's function technique [4].

The quasistatic magnetic hysteresis of ferromagnetic thin films grown on a vicinal substrate has been theoretically investigated by Monte Carlo simulations within a 2D model [5]. Structural and magnetic properties of two dimensional FeCo orders alloys deposited on W(110) substrates have been studied using first principles band structure theory [6]. Previously strontium ferrite and nickel ferrite films were synthesized using sputtering by us [7,8]. In addition, lithium mixed ferrite films were fabricated using pulsed laser deposition [9]. For all these films, the coercivity of film increased due to the stress induced anisotropy. The change of coercivity due to the stress induced anisotropy was qualitatively calculated for all these films. The calculated values of the change of coercivity agreed with the experimentally found values. So the stress induced anisotropy plays a major role in magnetic thin fabrications. Previously the Heisenberg Hamiltonian was employed to investigate the second order perturbed energy of ultrathin ferromagnetic films, thick ferromagnetic films, unperturbed energy of spinel ferrite films, second order perturbed energy of thick ferromagnetic films, third order perturbed energy of thick spinel ferrite, third order perturbed energy of thin spinel ferrite, second order perturbed energy of thick ferrite and the spin reorientation of barium hexa-ferrite [10–17].

Many other researchers have used Heisenberg Hamiltonian to solve the problems of magnetic thin films. Ferromagnetic thin films have been previously studied using the Heisenberg Hamiltonian with spin exchange interaction, magnetic dipole interaction, applied magnetic field, second and fourth order magnetic

 

anisotropy [18–20]. Magnetization reversal and domain structure in thin magnetic films have been theoretically investigated [21]. In-plane dipole coupling anisotropy of a square ferromagnetic Heisenberg monolayer has been described using Heisenberg Hamiltonian [22]. Effect of the interracial coupling on the magnetic ordering in ferro-antiferromagntic bilayers has been studied using Heisenberg Hamiltonian [23].

## MODEL

Following modified Hamiltonian was used as the model.

$$H = -J\sum_{m,n}\vec{S}_m.\vec{S}_n + \omega\sum_{m\neq n}\left(\frac{\vec{S}_m.\vec{S}_n}{r_{mn}^{\ 3}} - \frac{3(\vec{S}_m.\vec{r}_{mn})(\vec{r}_{mn}.\vec{S}_n)}{r_{mn}^{\ 5}}\right) - \sum_m D_{\lambda_m}^{\ (2)}(S_m^{\ z})^2 - \sum_m D_{\lambda_m}^{\ (4)}(S_m^{\ z})^4 - \sum_m \vec{H}.\vec{S}_m - \sum_m K_s Sin2\theta_m \quad (1)$$

Here J is spin exchange interaction, ω is the strength of long range dipole interaction, θ is azimuthal angle of spin, $D_m^{(2)}$ and $D_m^{(4)}$ are second and fourth order anisotropy constants, $H_{in}$ and $H_{out}$ are in plane and out of plane applied magnetic fields, $K_s$ is stress induced anisotropy constant, n and m are spin plane indices, and N is total number of layers in film. When the stress applies normal to the film plane, the angle between $m^{th}$ spin and the stress is $\theta_m$. In this 2-D model, only the x any components of the spin are considered. After considering only the x and y components of the spin, the total energy per unit spin can be deduced to the following equation;

$$E(\theta) = -\frac{1}{2}\sum_{m,n=1}^{N}\left[\left(JZ_{|m-n|} - \frac{\omega}{4}\Phi_{|m-n|}\right)\cos(\theta_m-\theta_n) - \frac{3\omega}{4}\Phi_{|m-n|}\cos(\theta_m+\theta_n)\right] - \sum_{m=1}^{N}\left(D_m^{(2)}\cos^2\theta_m + D_m^{(4)}\cos^4\theta_m + H_{in}\sin\theta_m + H_{out}\cos\theta_m\right) + \sum_{m,n=1}^{N}\frac{N_d}{\mu_0}\cos(\theta_m-\theta_n) - K_s\sum_{m=1}^{N}\sin 2\theta_m \quad (2)$$

with m (or n) $Z_{|m-n|}, \phi_{|m-n|}, \theta_m (or\ \theta_n)$, *N*, $H_{in}$ and $H_{out}$ being indices of layers, number of nearest spin neighbors, constant arising from summation of dipole interactions, azimuthal angles of spins, total number of layers, in plane applied field and out of plane applied field, respectively. For nonoriented films above angles $\theta_m$ and $\theta_n$ measured with film normal can be expressed in forms of $\theta_m = \theta + \varepsilon_m$ and $\theta_n = \theta + \varepsilon_n$, and above energy can be expanded up to the third order of ε as following. Here $\varepsilon_m$ (or $\varepsilon_n$) is a small perturbation of the angle.

$$E(\theta)=E_0+E(\varepsilon)+E(\varepsilon^2)+E(\varepsilon^3) \quad (3)$$

Here $E_0 = -\frac{1}{2}\sum_{m,n=1}^{N}\left(JZ_{|m-n|} - \frac{\omega}{4}\Phi_{|m-n|}\right) + \frac{3\omega}{8}\cos 2\theta\sum_{m,n=1}^{N}\Phi_{|m-n|} - \cos^2\theta\sum_{m=1}^{N}D_m^{(2)} - \cos^4\theta\sum_{m=1}^{N}D_m^{(4)} - N\left(H_{in}\sin\theta + H_{out}\cos\theta - \frac{N_d}{\mu_0} + K_s\sin 2\theta\right)$

$$E(\varepsilon) = -\frac{3\omega}{8}\sin 2\theta\sum_{m,n=1}^{N}\Phi_{|m-n|}(\varepsilon_m+\varepsilon_n) + \sin 2\theta\sum_{m=1}^{N}D_m^{(2)}\varepsilon_m + 2\cos^2\theta\sin 2\theta\sum_{m=1}^{N}D_m^{(4)}\varepsilon_m$$

$$-H_{in}\cos\theta\sum_{m=1}^{N}\varepsilon_m+H_{out}\sin\theta\sum_{m=1}^{N}\varepsilon_m-2K_s\cos 2\theta\sum_{m=1}^{N}\varepsilon_m$$

$$\text{E}(\varepsilon^2)=\frac{1}{4}\sum_{m,n=1}^{N}(JZ_{|m-n|}-\frac{\omega}{4}\Phi_{|m-n|})(\varepsilon_m-\varepsilon_n)^2-\frac{3\omega}{16}\cos 2\theta\sum_{m,n=1}^{N}\Phi_{|m-n|}(\varepsilon_m+\varepsilon_n)^2$$

$$-(\sin^2\theta-\cos^2\theta)\sum_{m=1}^{N}D_m{}^{(2)}\varepsilon_m{}^2+2\cos^2\theta(\cos^2\theta-3\sin^2\theta)\sum_{m=1}^{N}D_m{}^{(4)}\varepsilon_m{}^2$$

$$+\frac{H_{in}}{2}\sin\theta\sum_{m=1}^{N}\varepsilon_m{}^2+\frac{H_{out}}{2}\cos\theta\sum_{m=1}^{N}\varepsilon_m{}^2-\frac{N_d}{2\mu_0}\sum_{m,n=1}^{N}(\varepsilon_m-\varepsilon_n)^2$$

$$+2K_s\sin 2\theta\sum_{m=1}^{N}\varepsilon_m{}^2$$

$$E(\varepsilon^3)=\frac{\omega}{16}\sin 2\theta\sum_{m,n=1}^{N}(\varepsilon_m+\varepsilon_n)^3\phi_{|m-n|}-\frac{4}{3}\cos\theta\sin\theta\sum_{m=1}^{N}D_m{}^{(2)}\varepsilon_m{}^3$$

$$-4\cos\theta\sin\theta(\frac{5}{3}\cos^2\theta-\sin^2\theta)\sum_{m=1}^{N}D_m{}^{(4)}\varepsilon_m{}^3+\frac{H_{in}}{6}\cos\theta\sum_{m=1}^{N}\varepsilon_m{}^3$$

$$-\frac{H_{out}}{6}\sin\theta\sum_{m=1}^{N}\varepsilon_m{}^3+\frac{4K_s}{3}\cos 2\theta\sum_{m=1}^{N}\varepsilon_m{}^3 \qquad (4)$$

$$\sum_{m=1}^{N}\varepsilon_m=0$$

After using the constraint , $\text{E}(\varepsilon)=\vec{\alpha}.\vec{\varepsilon}$

Here $\vec{\alpha}(\varepsilon)=\vec{B}(\theta)\sin 2\theta$ are the terms of matrices with

$$B_\lambda(\theta)=-\frac{3\omega}{4}\sum_{m=1}^{N}\Phi_{|\lambda-m|}+D_\lambda{}^{(2)}+2D_\lambda{}^{(4)}\cos^2\theta \qquad (5)$$

Also $E(\varepsilon^2)=\frac{1}{2}\vec{\varepsilon}.C.\vec{\varepsilon}$

Here the elements of matrix C can be given as following;

$$C_{mn}=-(JZ_{|m-n|}-\frac{\omega}{4}\Phi_{|m-n|})-\frac{3\omega}{4}\cos 2\theta\Phi_{|m-n|}+\frac{2N_d}{\mu_0}$$

$$+\delta_{mn}\{\sum_{\lambda=1}^{N}[JZ_{|m-\lambda|}-\Phi_{|m-\lambda|}(\frac{\omega}{4}+\frac{3\omega}{4}\cos 2\theta)]-2(\sin^2\theta-\cos^2\theta)D_m{}^{(2)}$$

$$+4\cos^2\theta(\cos^2\theta-3\sin^2\theta)D_m{}^{(4)}+H_{in}\sin\theta+H_{out}\cos\theta-\frac{4N_d}{\mu_0}+4K_s\sin 2\theta\} \qquad (6)$$

And also third order can be expressed as the

$E(\varepsilon^3)=\varepsilon^2\beta.\vec{\varepsilon}$

Here matrix elements of matrix β can be given as following;

$$\beta_{mn}=\frac{3\omega}{8}\sin 2\theta\Phi_{|m-n|}+\delta_{mn}\{\frac{\omega}{8}\sin 2\theta[A_m-\Phi_0]-\frac{4}{3}\cos\theta\sin\theta D_m{}^{(2)}$$

$$-4\cos\theta\sin\theta(\frac{5}{3}\cos^2\theta-\sin^2\theta)D_m{}^{(4)}+\frac{H_{in}}{6}\cos\theta-\frac{H_{out}}{6}\sin\theta$$

$$+\frac{4K_s}{3}\cos 2\theta\} \qquad (7)$$

Also $\beta_{nm}=\beta_{mn,}$ and matrix β is symmetric.
By substituting all the terms, total energy can be expressed as

$$E(\theta)=E_0+\vec{\alpha}.\vec{\varepsilon}+\frac{1}{2}\vec{\varepsilon}.C.\vec{\varepsilon}+\varepsilon^2\beta.\vec{\varepsilon}$$

At the minimum energy (the stable state or the energetically favorable state), the derivative of above E(θ) with respect to ε will be zero. Using that condition, ε can be found. After substituting that ε in above equation of E(θ), following equation can be derived.

$$E(\theta)=E_0-\frac{1}{2}\vec{\alpha}.C^{+}.\vec{\alpha}-(C^{+}\alpha)^2\vec{\beta}(C^{+}\alpha) \quad (8)$$

The total magnetic energy have been calculated only for three layers (N=3), and the equation have been proved under the assumption of $D_1^{(2)}=D_2^{(2)}=D_3^{(2)}$ and $D_1^{(4)}=D_2^{(4)}=D_3^{(4)}$.

Following equation has been used to calculate the elements of matrix $C^{+}$.

$$C.C^{+}=1-\frac{E}{N} \quad (9)$$

Here E is the matrix with all elements given by $E_{mn}=1$.

## RESULTS AND DISCUSSION

Previously, the magnetic energy of ferromagnetic films with two and three layers has been found using the third order perturbed Heisenberg Hamiltonian with spin exchange interaction, second order magnetic anisotropy and stress induced anisotropy terms only to avoid tedious calculations [17]. Using a MATLAB computer program, the third order perturbed magnetic energy equation with all the seven magnetic parameters could be solved. The data of third order perturbed magnetic energy equation with all seven terms for bcc (001) structured ferromagnetic film with three layers (N=3) is presented in this manuscript.

For bcc (001) lattice $Z_0=0$, $Z_1=4$, $Z_2=0$, $\Phi_0=5.8675$ and $\Phi_1=2.7126$ [18].

The 3-D plots of $\frac{E(\theta)}{\omega}$ versus θ and $\frac{K_s}{\omega}$ is given in Figure 1. Other parameters were kept at $\frac{D_m^{(2)}}{\omega}=30, \frac{D_m^{(4)}}{\omega}=20, \frac{J}{\omega}=\frac{H_{in}}{\omega}=\frac{H_{out}}{\omega}=\frac{N_d}{\omega}=10$

According to this figure, several easy and hard directions can be observed for each value of stress induced anisotropy. Hard directions with two different energies could be observed.

When $\frac{K_s}{\omega}$= 3.5, 8, 13.5, 18, ---- etc. hard directions of magnetizations with higher energy can be seen. At each case, hard direction of magnetization appears at θ=7 radians. When $\frac{K_s}{\omega}$= 11, 21, ---- etc. hard directions of magnetizations with lower energy can be seen. Similarly easy directions with two different energies could be observed. When $\frac{K_s}{\omega}$=10, 20, 30, ---- etc. easy directions of magnetizations with lower energy can be seen.

When $\frac{K_s}{\omega}$=7, 17, 27, ---- etc. easy directions of magnetizations with higher energy can be seen. For each case, easy direction can be observed at θ= 4 radians. According to our previous experimental data, stress induced anisotropy is crucial in the deposition of magnetic thin films [7–10].

3-D plot of $\frac{E(\theta)}{\omega}$ versus θ and $\frac{H_{out}}{\omega}$ is shown in Figure 2. Other parameters were kept at $\frac{D_m^{(2)}}{\omega}=30, \frac{D_m^{(4)}}{\omega}=20, \frac{K_s}{\omega}=\frac{J}{\omega}=\frac{H_{in}}{\omega}=\frac{N_d}{\omega}=10$

Several peaks corresponding to easy and hard directions can be observed. Again hard directions with two different energies could be observed. When $\frac{H_{out}}{\omega}$ =6, 11, 16, ------etc. hard directions of magnetizations with higher energy can be seen. When $\frac{H_{out}}{\omega}$ =3, 8, 13, ------ etc. hard directions of magnetizations with lower energy can be seen. Hard direction could be observed at θ=3 radians. Similarly easy directions with two different energies could be observed. When $\frac{H_{out}}{\omega}$ =2, 7, 12, ------etc. easy directions of magnetizations with lower energy

can be seen. When $\frac{H_{out}}{\omega}$ =5, 15, 25, ------etc. easy directions of magnetizations with higher energy can be seen. Easy direction appears at θ=7 radians.

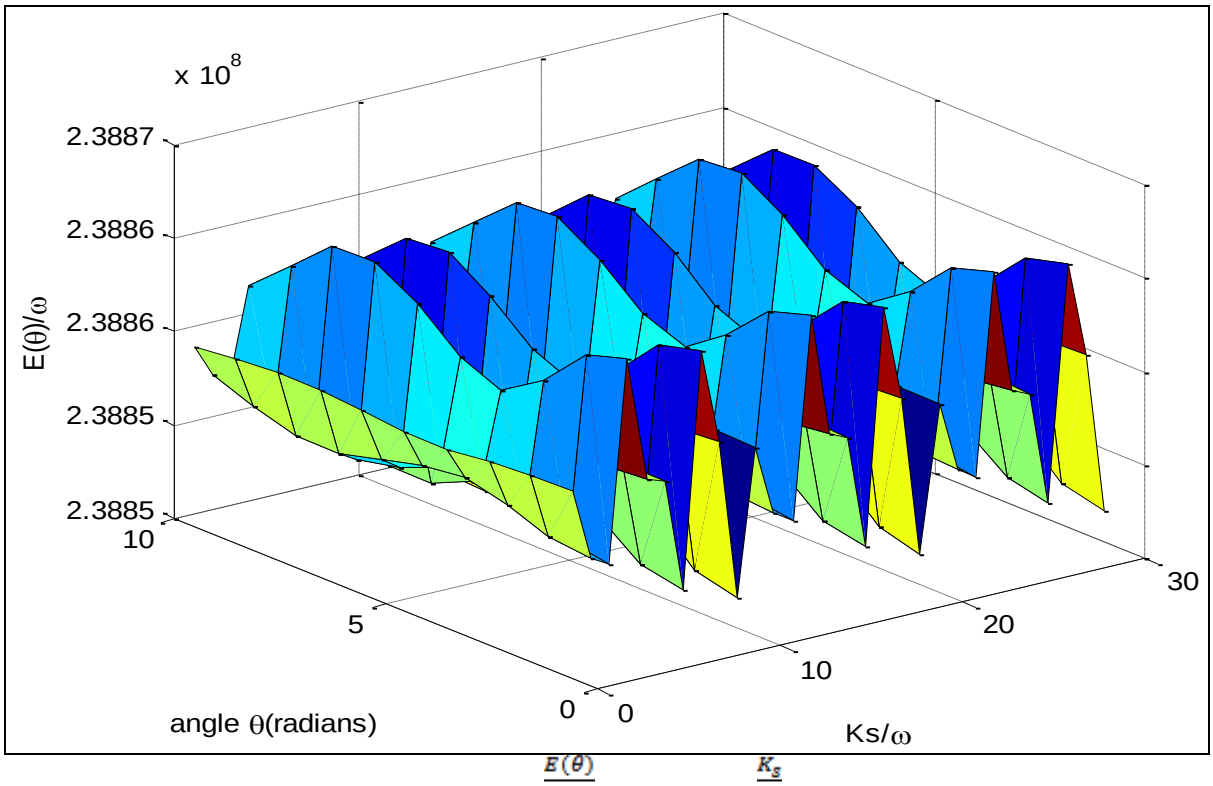


***Fig. 1:*** *3-D plot of* $\frac{E(\theta)}{\omega}$ *versus θ and* $\frac{K_s}{\omega}$ *for N=3.*

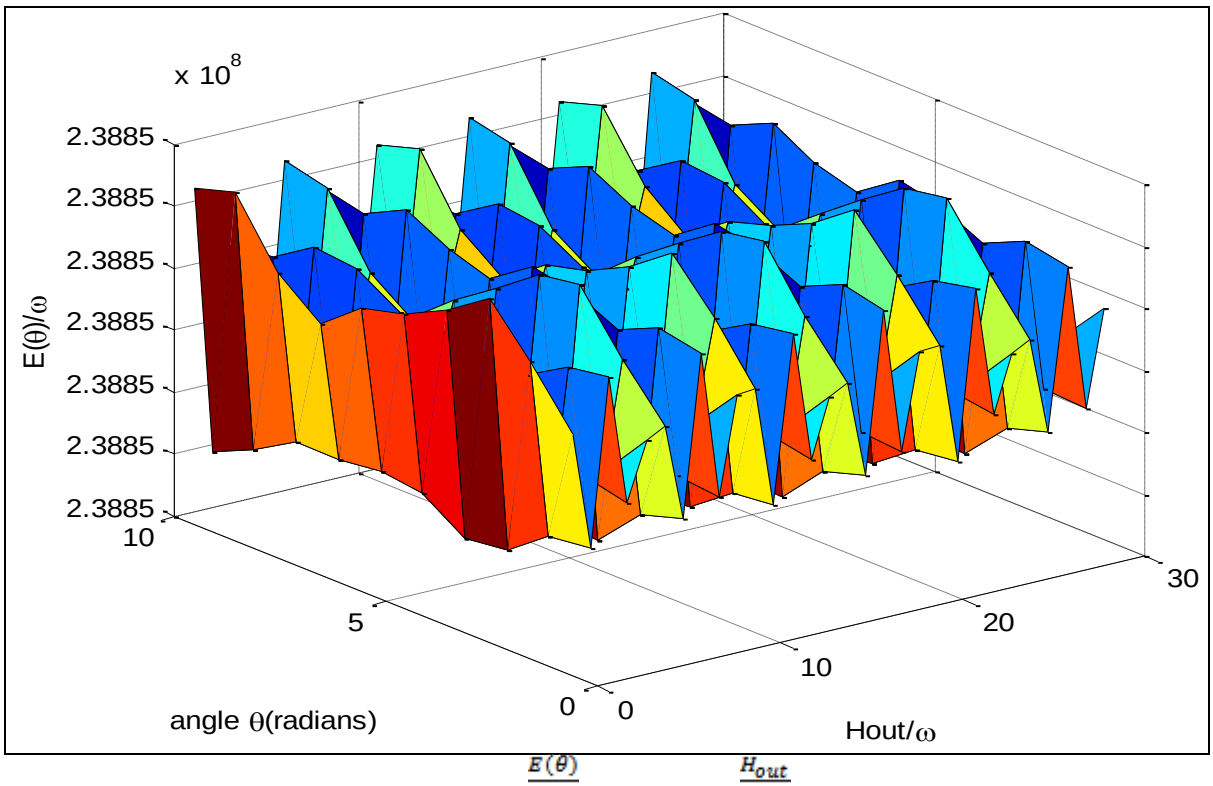


***Fig. 2:*** *3-D plot of* $\frac{E(\theta)}{\omega}$ *versus θ and* $\frac{H_{out}}{\omega}$ *for N=3.*

Figure 3 shows the 3-D plot of $\frac{E(\theta)}{\omega}$ versus θ and $\frac{N_d}{\omega}$. Other parameters were kept at $\frac{D_m^{(2)}}{\omega}=30, \frac{D_m^{(4)}}{\omega}=20, \frac{K_s}{\omega}=\frac{J}{\omega}=\frac{H_{in}}{\omega}=\frac{H_{out}}{\omega}=10$

Hard directions of magnetizations can be observed at $\frac{N_d}{\omega}$ =10, 20, 30, ------- etc.

Easy directions of magnetizations can be observed at $\frac{N_d}{\omega}$ =11, 21, ------- etc.

Figure 4 shows the 3-D plot of $\frac{E(\theta)}{\omega}$ versus θ and $\frac{J}{\omega}$.

Other parameters were kept at $\frac{D_m^{(2)}}{\omega}=30, \frac{D_m^{(4)}}{\omega}=20, \frac{K_s}{\omega}=\frac{H_{in}}{\omega}=\frac{H_{out}}{\omega}=\frac{N_d}{\omega}=10$

Several peaks can be observed corresponding to easy and hard directions of magnetization. Hard directions of magnetization can be observed at $\frac{J}{\omega}$ =1, 11, 21, ----etc.

Easy directions of magnetization appear at $\frac{J}{\omega}$ =10, 20, 30, -------etc. One hard direction of magnetization can be observed at θ=3 radians. Easy direction can be observed at θ=2 radians approximately.

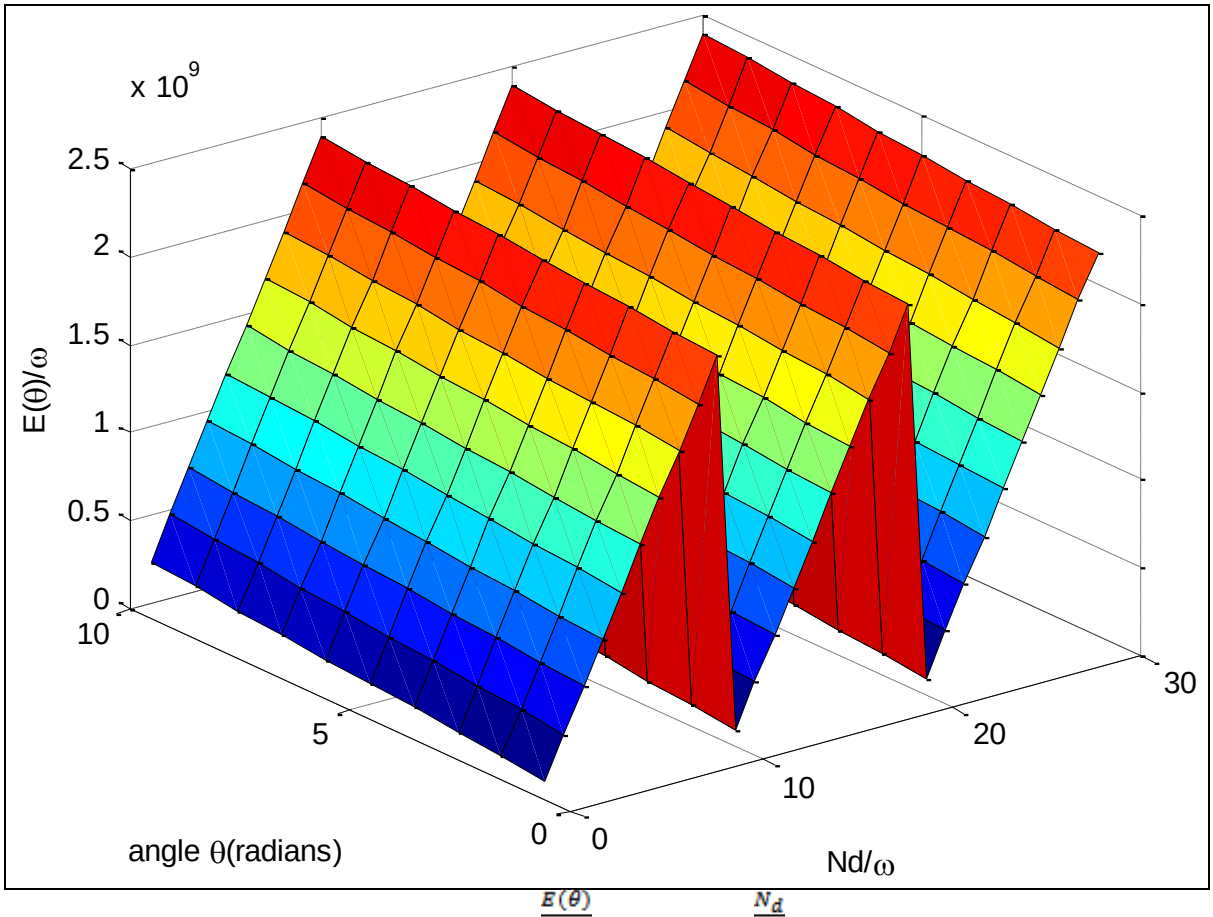


***Fig. 3:*** *3-D plot of* $\frac{E(\theta)}{\omega}$ *versus θ and* $\frac{N_d}{\omega}$ *for N=3.*

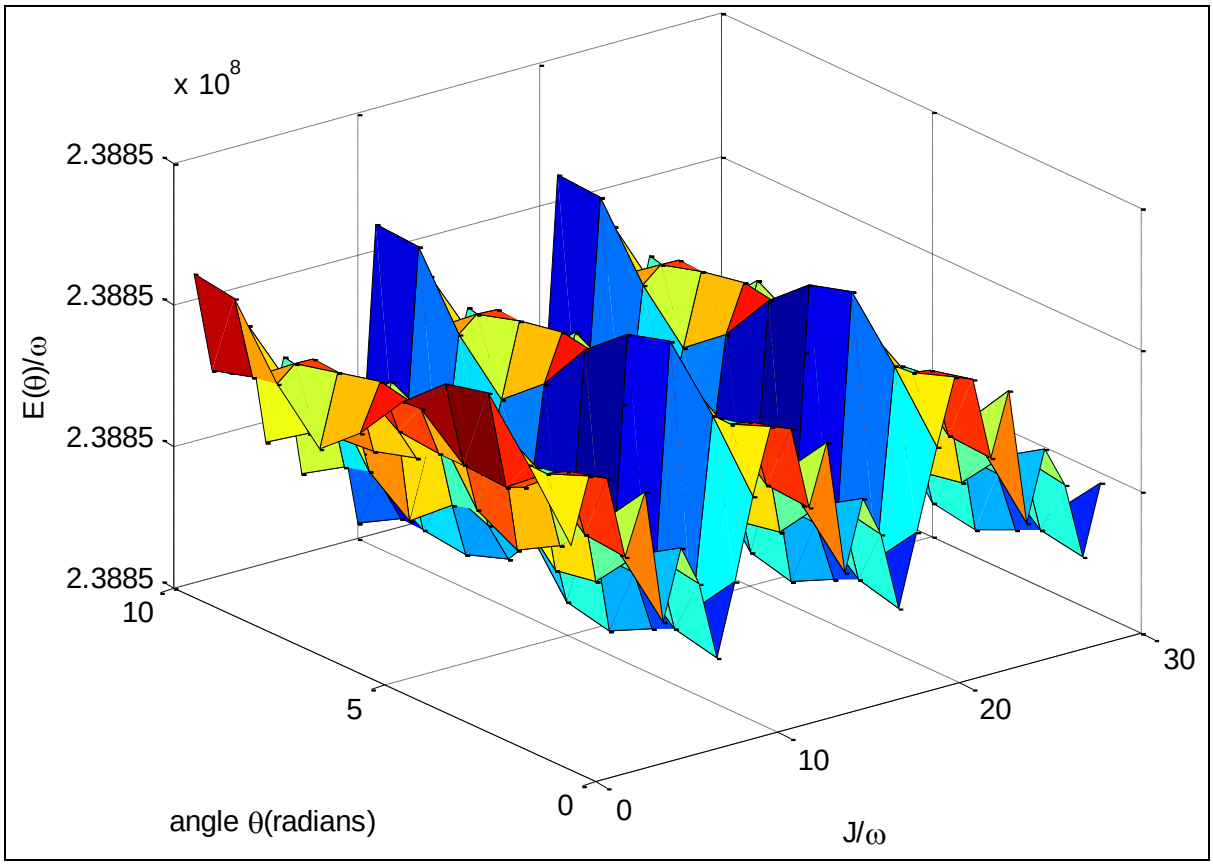


***Fig. 4:*** *3-D plot of* $\frac{E(\theta)}{\omega}$ *versus θ and* $\frac{J}{\omega}$ *for N=3.*

## CONCLUSION

According to 3-D plots of $\frac{E(\theta)}{\omega}$ versus θ and $\frac{K_s}{\omega}$, hard directions of magnetizations with higher energy can be seen at $\frac{K_s}{\omega}$ = 3.5, 8, 13.5, 18, ----etc. and hard directions of magnetizations with lower energy can be seen at $\frac{K_s}{\omega}$ = 11, 21, ----etc. At each case, hard direction of magnetization appears at θ=7 radians. Easy directions of magnetizations with lower energy can be seen at $\frac{K_s}{\omega}$=10, 20, 30, ----etc. Easy directions of magnetizations with higher energy can be seen at $\frac{K_s}{\omega}$=7, 17, 27, ----etc. For each case, easy direction can be observed at θ= 4 radians. Similarly several easy and hard directions were observed for $\frac{H_{out}}{\omega}$, $\frac{N_d}{\omega}$ and $\frac{J}{\omega}$. Previously the third order perturbed Heisenberg Hamiltonian with only three magnetic energy parameters was solved for simple cubic ultra thin ferromagnetic films with two and three layers by us [17]. However, only few peaks could be observed for the graph of $\frac{K_s}{J}$ in that case.

## REFERENCES

1. Anna Radomska, Tadeusz Balcerzak, *Cent Eur J Phys*. 2003; 1(1): 100–117p.
2. James C. Cates, Chester Alexander Jr., *J Appl Phys.* 1994; 75: 6754–6756p.
3. Ernst A. *et al. J Phys Condens Matt.* 2000; 12(26): 5599–5606p.
4. St Kovachev, Wesselinowa JM. *J Phys: Condens matt.* 2009: 21(22): 225007p.
5. Zhao D, *et al. J Appl Phys.* 2002; 91(5): 3150–3153p.
6. Spisak D, Hafner J. *J Mag Mag Mat.* 2005; 286: 386–389p.
7. Hegde H, *et al. J Appl Phys.* 1994; 75(10): 6640–6642p.

  

8. Samarasekara P. *Chinese J Phys.* 2003; 41(1): 70–74p.
9. Samarasekara P. *Chinese J Phys.* 2002; 40(6): 631–636p.
10. Samarasekara P., *Elec. J. Theo. Phys.* 2006; 3(11): 71–83p.
11. Samarasekara P. *Chinese J Phys.* 2006; 44(5): 377–386p.
12. Samarasekara P. *Elec J Theo Phys.* 2007; 4(15): 187–200p.
13. Samarasekara P, De Silva SNP, *Chinese J Phys.* 2007; 45(2-I): 142–150p.
14. Samarasekara P. *Inventi Rapid: Algorithm J.* 2011; 2(1): 1–3p.
15. Samarasekara P. William A. Mendoza, *GESJ: Phys*. 2011; 1(5): 15–24p.
16. Samarasekara P. *GESJ: Phys.* 2010; 1(3): 46–49p.
17. Samarasekara P, Udara Saparamadu, *GESJ: Phys.* 2013; 1(9): 10–15p.
18. Usadel KD, Hucht A. *Phys Rev B.* 2002; 66: 024419–1p.
19. Hucht A, Usadel KD. *Phys Rev B.* 1997; 55: 12309–1p.
20. Hucht A, Usadel KD. *J Mag Mag Mat.* 1999; 203(1): 88–90p.
21. Nowak U. *IEEE T Magnet.* 1995; 31(6-2): 4169–4171p.
22. Dantziger M, *et al. Phys Rev B.* 2002; 66: 094416p.
23. Shan-Ho Tsai, *et al. J Appl Phys*. 2003; 93(10): 8612–8614p.

**Cite this Article**
Samarasekara P, Yapa NUS. Third Order Perturbed Heisenberg Hamiltonian of BCC Ferromagnetic Ultra-Thin Films. *Research & Reviews: Journal of Physics.* 2016; 5(2): 23–30p.